# On the Reliability of Majority-Vote Pseudo-Labels in Test-Time Reinforcement Learning

**Haoyu Wang**[1], **Ru Wang**[3], **Yuanyuan Wang**[1], **Jiaxian Guo**[3], **Mingming Gong**[1,2]

[1]Mohamed bin Zayed University of Artificial Intelligence
[2]The University of Melbourne
[3]The University of Tokyo

arXiv:2611.09872v1 [cs.AI] 6 Nov 2026

**Abstract**

Test-time reinforcement learning (TTRL) adapts pretrained language models to unlabeled target-domain data using self-generated pseudo-labels, whose reliability remains poorly understood. We analyze majority-vote supervision for TTRL with online Direct Preference Optimization (DPO) and decompose its error into population-majority bias and prompt-dependent finite-rollout variation. Because population-majority bias is generally unidentifiable without external supervision, we focus on mitigating the downstream effects of finite-rollout variation. We propose *Prompt-Conditional Distributionally Robust DPO (PC-Dr.DPO)*, which conditions within-prompt robust reweighting on observed vote reliability to make updates from sampling-sensitive prompts more conservative. We further introduce a cache-based mechanism to reduce self-supervised forgetting during online adaptation. Across six mathematical and knowledge-intensive reasoning benchmarks and five model backbones, PC-Dr.DPO matches or outperforms the strongest TTRL baseline in 24 of 30 settings.

## 1 Introduction

Large language models (LLMs) have achieved strong performance across reasoning, planning, and knowledge-intensive tasks through large-scale pretraining and post-training alignment (OpenAI 2026; Google 2026; DeepSeek-AI 2026; Moonshot AI 2026; Qwen Team 2026). However, conventional post-training is predominantly *offline*: model parameters are fixed before deployment and cannot adapt to shifts in the test-time input distribution. This limitation is especially important in new or specialized domains, where labeled adaptation data and reliable external verifiers may be unavailable. It motivates test-time learning methods that adapt LLMs using unlabeled target-domain inputs and signals generated by the model itself.

**Test-time reinforcement learning.** Test-time reinforcement learning (TTRL) adapts a model on unlabeled target-domain prompts using self-generated rewards (Zuo et al. 2025). Existing approaches construct such rewards from either *certainty-based* signals, including prediction entropy and self-certainty (Prabhudesai et al. 2025; Zhao et al. 2025), or *ensemble-based* signals, including majority-vote consistency and agreement across alternative views of an input (Zuo et al. 2025; Zhang et al. 2025; Wang et al. 2025). Although these methods can improve reasoning without ground-truth labels, their success depends critically on the reliability of the resulting self-supervision.

Despite encouraging empirical results, this reliability remains incompletely understood. Prior work reports improvements even under imperfect or spurious rewards (Shao et al. 2025), whereas other studies highlight risks such as memorization and contamination (Wu et al. 2025b). Recent work further documents failure and collapse patterns in TTRL (He et al. 2026). Nevertheless, the lack of a formal framework characterizing when self-generated pseudo-labels are reliable limits the principled design of test-time adaptation algorithms.

In this work, we study majority-vote pseudo-labels for TTRL with online Direct Preference Optimization (DPO) (Rafailov et al. 2024; Pang et al. 2024; Ko et al. 2024). We identify two distinct sources of majority-vote error: (i) *population-majority bias*, which occurs when the behavior policy's population-modal answer is incorrect, and (ii) *finite-rollout variation*, which occurs when the sampled majority differs from the population mode. The former cannot generally be identified or corrected without external supervision. The latter instead reflects sampling sensitivity and varies across prompts according to how decisively the behavior policy favors its modal answer over competing answers.

This prompt-level heterogeneity is important for preference construction. Figure 1 shows the distribution of the observed modal-answer fraction for Qwen2.5-Math-1.5B-Instruct on AMC. Although some prompts produce nearly unanimous rollout groups, others exhibit highly fragmented answer distributions. For the latter prompts, the selected pseudo-label is more sensitive to the particular rollout sample and may change under resampling.

Existing noise-robust preference optimization methods typically employ either a shared dataset-level noise model or a globally normalized robust objective over preference pairs (Mitchell 2023; Wu et al. 2025a). Consequently, they do not explicitly adapt the strength of robustness to the prompt-dependent reliability induced by finite-rollout sampling during test-time adaptation.

**Our approach: PC-Dr.DPO.** To address this mismatch, we propose *Prompt-Conditional Distributionally Robust DPO (PC-Dr.DPO)*. PC-Dr.DPO performs robust reweighting separately within each prompt's rollout group and adapts a prompt-specific robustness temperature using observed

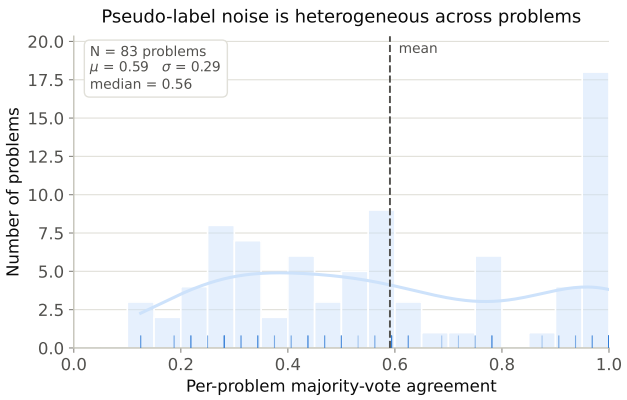



Figure 1: Distribution of prompt-level modal-answer agreement for Qwen2.5-Math-1.5B-Instruct on the 83-problem AMC benchmark. For each prompt $x$, we sample $m = 32$ rollouts and compute the fraction producing the most frequent final answer. The broad distribution indicates substantial prompt-level heterogeneity: values near one correspond to nearly unanimous rollout groups, whereas smaller values indicate fragmented answer distributions that are more sensitive to resampling.

majority-vote reliability as a proxy for sampling sensitivity. For low-reliability prompts, the resulting reweighting emphasizes preference pairs already better satisfied by the current policy, yielding more conservative updates that mitigate the downstream optimization effects of finite-rollout errors. We further introduce a cache-based stabilization mechanism to reduce self-supervised forgetting during long-horizon online adaptation.

**Our contributions are threefold:**

- We develop a theoretical framework that separates population-majority bias from finite-rollout variation and characterizes how majority-vote errors propagate into the generalization risk of models trained on pseudo-preferences with a DPO-style objective.
- We propose *PC-Dr.DPO*, which uses prompt-level vote reliability to adapt within-prompt robust reweighting and reduce the influence of sampling-sensitive pseudo-labels. We further introduce a cache-based mechanism to mitigate self-supervised forgetting.
- We evaluate PC-Dr.DPO across six mathematical and knowledge-intensive reasoning benchmarks and five model backbones, matching or outperforming the strongest TTRL baseline in 24 of 30 settings.

## 2 Preliminaries

We briefly review the learning setting and the preference-optimization objectives that our analysis and method build upon. We keep the discussion minimal and focus on the notation used throughout the paper.

### Problem Setup and RLVR Objective

Let $\pi_\theta$ denote a large language model parameterized by $\theta$, and let $\mathcal{D}$ be a dataset of question–answer pairs $(x, a)$. Given a prompt $x$, the model generates a response trajectory $y = (y_{t1}, \ldots, y_{tn}) \sim \pi_\theta(\cdot \mid x)$ autoregressively. We consider reasoning-style responses that contain intermediate steps (e.g., CoT (Wang et al. 2023)) and a final answer extracted by a deterministic function $\mathrm{ans}(\cdot)$.

In the standard reinforcement learning with verifiable rewards (RLVR) setting (DeepSeek-AI 2025), we assume access to a verifier that compares the extracted answer with the ground-truth answer $a$, yielding the binary reward $r(x, y; a) = \mathbf{1}\{\mathrm{ans}(y) = a\}$. Training with verifiable rewards is commonly formulated as KL-regularized policy optimization (Ouyang et al. 2022):

$$\max_{\pi_\theta} \mathbb{E}_{x\sim\mathcal{D}}\Big[\mathbb{E}_{y\sim\pi_\theta(\cdot|x)}\big[r(x,y)\big] - \tau\, D_{\mathrm{KL}}\big(\pi_\theta(\cdot \mid x) \,\|\, \pi_{\mathrm{ref}}(\cdot \mid x)\big)\Big]. \tag{1}$$

where $\pi_{\mathrm{ref}}$ is a reference policy (typically an SFT model) and $\tau > 0$ controls the strength of the KL regularization. In practice, several methods have been proposed to optimize (1), including PPO (Schulman et al. 2017), RLOO (Ahmadian et al. 2024), REMAX (Li et al. 2024), REINFORCE++ (Hu et al. 2025), and, most prominently, the GRPO family algorithms (Shao et al. 2024; Yu et al. 2025; Zheng et al. 2025).

**Test-time self-reward via majority voting.** Unlike standard RLVR, the TTRL setting considered here assumes neither ground-truth answers nor an external verifier at adaptation time. Instead, the model constructs self-supervision from its own rollouts. For each prompt $x$, the behavior policy samples $m$ independent responses $\{y_i\}_{i=1}^m$ with $y_i \sim \pi_b(\cdot \mid x)$ and forms the pseudo-label $\widehat{a}_{\mathrm{mv}}(x) = \arg\max_{a'} \sum_{i=1}^m \mathbf{1}\{\mathrm{ans}(y_i) = a'\}$ by majority voting over their extracted answers. This pseudo-label is used either to assign pseudo-rewards or to construct pseudo-preference pairs, treating matching rollouts as correct under the pseudo-label and the remaining rollouts as incorrect. Section 3 analyzes the reliability of this supervision under a DPO-style objective.

### Direct Preference Optimization

Rather than performing explicit policy-gradient optimization, Direct Preference Optimization (DPO) (Rafailov et al. 2024) provides a supervised objective for optimizing the KL-regularized reward maximization problem using winner–loser preference pairs.

Let $\mathcal{D}_{\mathrm{pref}}$ denote a dataset of preference tuples $(x, y_w, y_l)$, where $y_w \succ y_l$ indicates that $y_w$ is preferred to $y_l$ under prompt $x$. DPO minimizes

$$\mathcal{L}_{\mathrm{DPO}}(\theta) = -\mathbb{E}_{(x,y_w,y_l)\sim\mathcal{D}_{\mathrm{pref}}}\left[h_\theta(x, y_w, y_l)\right], \tag{2}$$

where the per-pair log-preference score is

$$h_\theta(x, y_w, y_l) = \log \sigma(\tau g_\theta(x, y_w, y_l)), \tag{3}$$

and

$$g_\theta(x, y_w, y_l) = \log \frac{\pi_\theta(y_w \mid x)}{\pi_{\mathrm{ref}}(y_w \mid x)} - \log \frac{\pi_\theta(y_l \mid x)}{\pi_{\mathrm{ref}}(y_l \mid x)}. \tag{4}$$

Here, $\sigma(\cdot)$ denotes the sigmoid function. We refer to $g_\theta$ as the DPO margin and to $h_\theta$ as the corresponding log-preference score.

Standard DPO operates on a fixed offline preference dataset. Online variants instead generate preference data iteratively from a behavior policy (Pang et al. 2024).

### Distributionally Robust DPO

Dr.DPO (Wu et al. 2025a) applies KL-based distributionally robust reweighting to reduce the influence of pairs that are inconsistent with the current policy-relative preference ordering. Let $s = (x, y_w, y_l)$ denote a preference sample and let $p$ be the empirical distribution over the preference dataset $\mathcal{D}_{\mathrm{pref}}$. Motivated by the dual form of a KL-constrained distributionally robust objective, Dr.DPO uses the fixed-temperature loss

$$\mathcal{L}_{\mathrm{DrDPO}}(\theta) = -\beta \log \mathbb{E}_{s\sim p}\left[\exp\left(\frac{h_\theta(s)}{\beta}\right)\right], \qquad \beta > 0, \tag{5}$$

where $h_\theta$ is the DPO log-preference score defined in Equation (3).

Define the current pairwise preference probability as

$$\nu_\theta(s) := \sigma(\tau g_\theta(s)),$$

so that $h_\theta(s) = \log \nu_\theta(s)$. The objective in Equation (5) induces the normalized exponential density ratio

$$w_\beta(s) = \frac{\exp(h_\theta(s)/\beta)}{\mathbb{E}_{s'\sim p}\left[\exp(h_\theta(s')/\beta)\right]}, \tag{6}$$

and hence

$$w_\beta(s) \propto \nu_\theta(s)^{1/\beta}.$$

The corresponding gradient is

$$\nabla_\theta \mathcal{L}_{\mathrm{DrDPO}}(\theta) = -\tau\, \mathbb{E}_{s\sim p}\left[w_\beta(s)\big(1-\nu_\theta(s)\big)\nabla_\theta g_\theta(s)\right]. \tag{7}$$

Smaller values of $\beta$ produce a sharper exponential tilt toward pairs with larger current preference probabilities. The KL-DRO derivation and a detailed analysis of the effect of $\beta$ on the resulting gradient are provided in Appendix A.1.

## 3 Analysis of Majority-Vote Pseudo-Labels

We first analyze the reliability of majority-vote pseudo-labels in test-time reinforcement learning by separating two sources of error: *population-majority bias*, where the modal answer under the behavior policy is incorrect, and *finite-rollout variation*, where a sampled majority differs from that population mode.

Throughout this section, we condition on a fixed behavior policy $\pi_b$ and adopt an i.i.d. preference-pair abstraction. Each sample $s = (x, y_w, y_l)$ is independently constructed from $m$ rollouts for a sampled prompt using majority-vote preference labeling. The analysis applies separately to each online update, with $\pi_b$ fixed to the rollout-generating policy at that update. Let $\mathcal{P}$ denote the resulting distribution over preference samples.

### Generalization under Approximate Preference Labels

Let $\mathcal{S}$ be the preference-sample space and $\mathcal{F} \subseteq \{f : \mathcal{S} \to \mathbb{R}\}$ a class of pairwise predictors. For $s = (x, y_w, y_l)$, let $z \in \{0, 1\}$ denote the latent true preference label, with $z = 1$ corresponding to $y_w \succ y_l$. Since the pair is ordered by the pseudo-labeling procedure, $z$ indicates whether the constructed ordering agrees with the true preference. We write $p^*(s) := (p^*(z = 1 \mid s), p^*(z = 0 \mid s))^\top \in \Delta_2$.

For DPO, the predictor is instantiated by the policy-relative margin

$$f_\theta(s) := \tau\left[\log \frac{\pi_\theta(y_w \mid x)}{\pi_{\mathrm{ref}}(y_w \mid x)} - \log \frac{\pi_\theta(y_l \mid x)}{\pi_{\mathrm{ref}}(y_l \mid x)}\right], \tag{8}$$

where $\tau > 0$ is the inverse-temperature parameter. The corresponding binary logistic loss is $\ell_{\mathrm{DPO}}(z, f) = -z \log \sigma(f) - (1 - z) \log \sigma(-f)$. Because the generalization result below requires a loss bounded in $[0, 1]$, we assume $|f(s)| \le M$ for every $f \in \mathcal{F}$ and $s \in \mathcal{S}$, and define $\ell(z, f) := \ell_{\mathrm{DPO}}(z, f)/\log(1 + e^M) \in [0, 1]$. This positive rescaling preserves empirical minimizers.

Let $\ell(f(s)) := (\ell(1, f(s)), \ell(0, f(s)))^\top$. The true population risk is defined using $p^*(s)$. Since $p^*(s)$ is unavailable at test time, empirical optimization instead uses the pseudo-preference distribution $\widehat{p}(s) \in \Delta_2$:

$$\begin{aligned} R(f) &:= \mathbb{E}_{s\sim\mathcal{P}}\left[p^*(s)^\top \ell(f(s))\right], \\ \widetilde{R}(f; S) &:= \frac{1}{N}\sum_{n=1}^{N} \widehat{p}(s_n)^\top \ell(f(s_n)), \end{aligned} \tag{9}$$

where $S = \{s_n\}_{n=1}^N \sim \mathcal{P}^N$.

Define the induced loss class and its covering complexity by

$$\begin{aligned} \widetilde{\mathcal{H}} &:= \left\{s \mapsto \widehat{p}(s)^\top \ell(f(s)) : \ f \in \mathcal{F}\right\}, \\ \widetilde{\mathcal{M}}_N &:= \mathcal{N}_\infty\left(\tfrac{1}{N}, \widetilde{\mathcal{H}}, 2N\right). \end{aligned} \tag{10}$$

Following Menon et al. (2021), $\mathcal{N}_\infty(\epsilon, \mathcal{H}, n)$ denotes the uniform $\ell_\infty$ covering number of $\mathcal{H}$ over samples of size $n$. For brevity, define the sample-dependent generalization term

$$\mathcal{G}_N(f, \delta; S) := O\left(\sqrt{\frac{\widetilde{\mathbb{V}}_N(f; S)\log(\widetilde{\mathcal{M}}_N/\delta)}{N}} + \frac{\log(\widetilde{\mathcal{M}}_N/\delta)}{N}\right), \tag{11}$$

where $\widetilde{\mathbb{V}}_N(f; S)$ is the empirical variance of $\{\widehat{p}(s_n)^\top \ell(f(s_n))\}_{n=1}^N$.

**Theorem 1** (Approximate preference distillation)**.** *For any $\delta \in (0, 1)$, with probability at least $1 - \delta$ over $S \sim \mathcal{P}^N$, every $f \in \mathcal{F}$ satisfies*

$$R(f) \le \widetilde{R}(f; S) + \frac{1}{2}\,\mathbb{E}_{s\sim\mathcal{P}}[\|\widehat{p}(s) - p^*(s)\|_1] + \mathcal{G}_N(f, \delta; S). \tag{12}$$

The second term in Equation (12) is the expected total-variation distance between the pseudo-preference and true conditional preference distributions. Unlike $\mathcal{G}_N(f, \delta; S)$, this mismatch need not vanish as $N$ increases and therefore contributes persistently to the bound when pseudo-label error is systematic. The complete proof is given in Appendix A.2.

### Majority-Vote Error Decomposition

To expose the central mechanism, we consider a binary answer space and assume deterministic ground-truth preferences. For any pair with distinct final answers, the true preference distribution $p^*(s)$ assigns probability one to the response whose extracted answer equals the ground-truth answer $a^\star(x)$. Define the per-rollout correctness probability and the population-majority answer under the behavior policy $\pi_b$ by

$$\begin{aligned} \rho_b(x) &:= \Pr_{\pi_b}(\mathrm{ans}(y) = a^\star(x) \mid x)\,, \\ a_b^\infty(x) &:= \arg\max_a \Pr_{\pi_b}(\mathrm{ans}(y) = a \mid x)\,. \end{aligned} \tag{13}$$

In the binary setting, $a_b^\infty(x) = a^\star(x)$ when $\rho_b(x) > 1/2$, whereas the population majority is incorrect when $\rho_b(x) < 1/2$. We assume that the rollout count $m$ is odd, so the sampled majority is unique, and adopt a fixed tie-breaking rule for the population boundary case $\rho_b(x) = 1/2$.

Given rollouts $y_1, \ldots, y_m \overset{\text{i.i.d.}}{\sim} \pi_b(\cdot \mid x)$, define the sampled-majority answer by

$$\widehat{a}_{m,b}(x) := \arg\max_a \sum_{i=1}^{m} \mathbf{1}\{\mathrm{ans}(y_i) = a\}\,. \tag{14}$$

A response agreeing with $\widehat{a}_{m,b}(x)$ is treated as the winner, whereas a response containing the alternative answer is treated as the loser. Thus, the pseudo-preference distribution assigns probability one to the constructed ordering, so $\widehat{p}(s) = (1,0)^\top$.

Define the conditional majority-vote error probability by

$$U_{m,b}(x) := \Pr(\widehat{a}_{m,b}(x) \neq a^\star(x) \mid x)\,, \tag{15}$$

Under the binary deterministic-preference abstraction, the expected total-variation term in Theorem 1 equals $\mathbb{E}_x[U_{m,b}(x)]$, as shown in Appendix A.3. Consequently, with the same probability $1-\delta$, every $f \in \mathcal{F}$ satisfies

$$R(f) \le \widetilde{R}(f;S) + \mathbb{E}_x[U_{m,b}(x)] + \mathcal{G}_N(f,\delta;S), \tag{16}$$

where the expectation is taken with respect to the prompt marginal induced by $\mathcal{P}$.

### Population Bias and Finite-Rollout Variation

We now decompose the majority-vote error into population-majority bias and finite-rollout variation:

$$\begin{aligned} B_b(x) &:= \mathbf{1}\left\{a_b^\infty(x) \neq a^\star(x)\right\}, \\ V_{m,b}(x) &:= \Pr(\widehat{a}_{m,b}(x) \neq a_b^\infty(x) \mid x)\,. \end{aligned} \tag{17}$$

**Proposition 1** (Exact majority-error decomposition)**.** *Under the binary-answer abstraction, for every prompt $x$,*

$$\begin{aligned} U_{m,b}(x) &= \big(1 - B_b(x)\big)V_{m,b}(x) + B_b(x)\big(1 - V_{m,b}(x)\big) \\ &= B_b(x) + \big(1 - 2B_b(x)\big)V_{m,b}(x). \end{aligned} \tag{18}$$

**Lemma 1** (Majority-vote concentration)**.** *For every prompt $x$ with $\rho_b(x) \neq 1/2$,*

$$V_{m,b}(x) \le \exp\Big(-2m\,\big|\rho_b(x) - \tfrac{1}{2}\big|^2\Big)\,. \tag{19}$$

Combining Proposition 1 and Lemma 1, for any $\gamma > 0$,

$$\begin{aligned} \rho_b(x) \ge \tfrac{1}{2} + \gamma &\Longrightarrow U_{m,b}(x) \le e^{-2m\gamma^2}, \\ \rho_b(x) \le \tfrac{1}{2} - \gamma &\Longrightarrow U_{m,b}(x) \ge 1 - e^{-2m\gamma^2}. \end{aligned} \tag{20}$$

**Corollary 1** (Generalization under majority-vote supervision)**.** *Suppose that $|\rho_b(x) - 1/2| \ge \gamma > 0$ almost surely, and let*

$$\alpha_b := \Pr_x\big(\rho_b(x) < \tfrac{1}{2}\big) = \mathbb{E}_x[B_b(x)].$$

*Then*

$$|\mathbb{E}_x[U_{m,b}(x)] - \alpha_b| \le e^{-2m\gamma^2}. \tag{21}$$

*Consequently, with probability at least $1-\delta$ over $S \sim \mathcal{P}^N$, every $f \in \mathcal{F}$ satisfies*

$$R(f) \le \widetilde{R}(f;S) + \alpha_b + e^{-2m\gamma^2} + \mathcal{G}_N(f,\delta;S). \tag{22}$$

Proofs are provided in Appendix A.4–A.5.

**Interpretation.** For a fixed behavior policy, $\alpha_b$ captures population-majority bias and does not decrease with the rollout count $m$. By contrast, finite-rollout variation decays exponentially in $m$. Increasing $m$ can therefore stabilize the sampled majority but cannot correct an incorrect population majority. Appendix C.1 empirically illustrates this distinction using Qwen2.5-Math-1.5B-Instruct on AMC with $m \in \{16, 32, 64\}$.

## 4 Our Method: Prompt-Conditional Dr.DPO

The preceding analysis separates majority-vote error into population-majority bias and finite-rollout variation under a simplified binary-answer abstraction. Without external supervision, the former is generally unidentifiable: an incorrect but decisive population majority may still appear highly reliable. We therefore focus on mitigating the downstream optimization effects of finite-rollout variation. Our method uses observed vote concentration as a proxy for sampling sensitivity and adjusts the strength of robust reweighting separately for each prompt.

### Prompt-Conditional Robust Objective

Let $p$ denote the empirical distribution over preference samples $s = (x, y_w, y_l)$. Standard Dr.DPO applies a globally normalized exponential tilt with a shared temperature across all preference pairs. To account for prompt-dependent reliability, we instead consider the conditional uncertainty set

$$\mathcal{U} = \{q : q(x) = p(x),\ \mathrm{KL}(q(\cdot \mid x) \,\|\, p(\cdot \mid x)) \le \eta_x,\ \forall x\}\,.$$

This set keeps the prompt marginal fixed while permitting prompt-specific reweighting of the conditional pair distribution. Given the DPO score $h_\theta$ defined in Equation (3), the corresponding robust score is

$$\sup_{q \in \mathcal{U}} \mathbb{E}_{s\sim q}\left[h_\theta(s)\right]. \tag{23}$$

Because $q(x) = p(x)$, the inner optimization decomposes across prompts:

$$\mathbb{E}_{x\sim p(x)}\left[\sup_{q_x:\,\mathrm{KL}(q_x \| p(\cdot|x)) \le \eta_x} \mathbb{E}_{s\sim q_x}\left[h_\theta(s)\right]\right]. \tag{24}$$

Applying KL-ball duality to each conditional problem gives

$$\mathbb{E}_{x\sim p(x)}\left[\inf_{\beta_x>0}\left\{\beta_x\eta_x+\beta_x\log\mathbb{E}_{s\sim p(\cdot|x)}\left[\exp\left(\frac{h_\theta(s)}{\beta_x}\right)\right]\right\}\right]. \tag{25}$$

Let $\beta_x=\beta_x^\star(\eta_x)$ denote the prompt-specific dual temperature associated with the prescribed radius $\eta_x$. Following the fixed-temperature formulation of Dr.DPO, we hold $\beta_x$ fixed during the policy update and omit the additive term $\beta_x\eta_x$, which is independent of $\theta$. This yields the prompt-conditional score

$$\mathbb{E}_{x\sim p(x)}\left[\beta_x\log\mathbb{E}_{s\sim p(\cdot|x)}\left[\exp\left(\frac{h_\theta(s)}{\beta_x}\right)\right]\right]. \tag{26}$$

The temperature $\beta_x$ controls the sharpness of the conditional exponential tilt. Smaller values concentrate weight on pairs with larger current DPO scores, whereas larger values produce weights closer to uniform within the prompt group.

**Finite-sample objective.** At adaptation step $t$, rollouts are sampled from $\pi_{t-1}$, which also serves as the reference policy: $\pi_{\mathrm{ref}}=\pi_{t-1}$. For each prompt $x$, let

$$P_t(x)=\{s_{xi}\}_{i=1}^{N_x},\qquad s_{xi}=(x,y_{w,i},y_{l,i}),$$

denote the resulting preference pairs. The prompt-conditional objective is

$$\mathcal{L}_{\text{PC-DrDPO}}(\theta;x)=-\beta_x\log\left[\frac{1}{N_x}\sum_{i=1}^{N_x}\exp\left(\frac{h_\theta(s_{xi})}{\beta_x}\right)\right]. \tag{27}$$

Unlike standard Dr.DPO, which normalizes globally over preference pairs, Equation (27) normalizes within each prompt group. Let

$$\nu_{xi}:=\sigma(\tau g_\theta(s_{xi})),\qquad h_\theta(s_{xi})=\log\nu_{xi}.$$

The induced weights and gradient are

$$\overline{w}_{xi}(\beta_x)=\frac{\nu_{xi}^{1/\beta_x}}{\sum_{k=1}^{N_x}\nu_{xk}^{1/\beta_x}}, \tag{28}$$

$$\nabla_\theta\mathcal{L}_{\text{PC-DrDPO}}(\theta;x)=-\tau\sum_{i=1}^{N_x}\overline{w}_{xi}(\beta_x)(1-\nu_{xi})\nabla_\theta g_\theta(s_{xi}). \tag{29}$$

As $\beta_x\to 0^+$, the objective approaches $-\max_i h_\theta(s_{xi})$ and the weights concentrate on the highest-scoring pairs; as $\beta_x\to\infty$, the weights become uniform over $P_t(x)$.

## Reliability-Conditioned Temperature

For each prompt $x$, let $\{y_i\}_{i=1}^m \overset{\text{i.i.d.}}{\sim}\pi_{t-1}(\cdot\mid x)$, and let $\widehat{a}_{m,t-1}(x)$ denote the sampled modal-answer. We define

$$\kappa(x):=\frac{1}{m}\sum_{i=1}^m\mathbf{1}\left\{\mathrm{ans}(y_i)=\widehat{a}_{m,t-1}(x)\right\}. \tag{30}$$

The modal-answer fraction $\kappa(x)$ does not determine whether the resulting pseudo-label is correct. Instead, it serves as an observable proxy for finite-rollout stability.

We set

$$\beta_x=\beta_{\text{base}}\kappa(x),\qquad \beta_{\text{base}}>0. \tag{31}$$

Thus, weaker observed majorities receive smaller temperatures and sharper within-prompt reweighting, whereas stronger majorities receive smoother weights closer to uniform averaging. The temperature is computed from the rollout group and held fixed during policy differentiation.

**Proposition 2** (Effect of prompt-conditional temperature)**.** *Fix $\theta$ and a prompt group $P_t(x)=\{s_{xi}\}_{i=1}^{N_x}$. Let $\nu_{xi}:=\nu_\theta(s_{xi})$ and define*

$$A_x(\beta):=\sum_{i=1}^{N_x}\overline{w}_{xi}(\beta)(1-\nu_{xi}). \tag{32}$$

*Then $A_x(\beta)$ is nondecreasing in $\beta$. Moreover, if $\|\nabla_\theta g_\theta(s_{xi})\|\le G$ for all $i$, then*

$$\|\nabla_\theta\mathcal{L}_{\text{PC-DrDPO}}(\theta;x)\|\le\tau G A_x(\beta_x). \tag{33}$$

*Consequently, with the current pairwise scores held fixed, decreasing $\beta_x$ decreases this upper bound on the prompt-level update magnitude.*

The proof is provided in Appendix A.1. Intuitively, a smaller temperature places greater weight on pairs with larger $\nu_{xi}$, for which the residual factors $1-\nu_{xi}$ are smaller. This moderates the gradient-norm upper bound for prompts whose sampled majorities appear less stable.

## Cache-Based Stabilization Against Self-Forgetting

Some prompts become degenerate during online adaptation: all sampled rollouts produce the same final answer, so no valid winner–loser pair can be constructed and $P_t(x)=\emptyset$. We exclude such prompts from the preference update.

When a prompt first becomes degenerate, we cache its rollout completions, denoted by $\mathcal{C}(x)$. Because all cached completions share the same final answer, we denote this answer by $a_{\mathcal{C}}(x)$. If the prompt is encountered again and its new sampled-majority answer disagrees with $a_{\mathcal{C}}(x)$, we discard the newly generated pseudo-preference pairs and instead apply the cache loss

$$\mathcal{L}_{\text{cache}}(\theta;x)=-\frac{1}{|\mathcal{C}(x)|}\sum_{y\in\mathcal{C}(x)}\log\pi_\theta(y\mid x). \tag{34}$$

This replay-style safeguard discourages a later conflicting pseudo-label from overwriting previously stable self-supervision.

## Overall Objective and Update Rule

For a mini-batch of prompts $\mathcal{B}_t$, let $\mathcal{B}_{\text{cache}}$ denote the prompts that trigger the cache rule, and define

$$\mathcal{B}_{\text{norm}}:=\{x\in\mathcal{B}_t\setminus\mathcal{B}_{\text{cache}}:P_t(x)\neq\emptyset\}.$$

The complete update objective is

$$\begin{aligned}\mathcal{L}_t(\theta)=&\frac{1}{|\mathcal{B}_{\text{norm}}|}\sum_{x\in\mathcal{B}_{\text{norm}}}\mathcal{L}_{\text{PC-DrDPO}}(\theta;x)\\&+\mu\cdot\frac{1}{|\mathcal{B}_{\text{cache}}|}\sum_{x\in\mathcal{B}_{\text{cache}}}\mathcal{L}_{\text{cache}}(\theta;x),\end{aligned} \tag{35}$$

where $\mu \geq 0$ controls the relative weight of the cache loss. (When $\mathcal{B}_{\text{cache}} = \emptyset$, the second term is omitted.)

At each adaptation step, we perform one or more gradient updates on Equation (35) and set the resulting policy as $\pi_t$. Using $\pi_{\text{ref}} = \pi_{t-1}$ keeps each DPO update local to the behavior policy that generated the corresponding rollout data.

**Trajectory-score-based answer selection.** Majority voting over discrete answers ignores within-answer heterogeneity. To incorporate the model's internal preference signal, we compute an *implicit DPO score* for each rollout using successive-policy likelihood ratios. At update step $t \geq 2$, we treat $\pi_{t-2}$ as a lagged reference and define

$$r_t(y \mid x) := \log \frac{\pi_{t-1}(y \mid x)}{\pi_{t-2}(y \mid x)}. \tag{36}$$

We aggregate these scores by extracted final answer and select $\widehat{a}^{\text{score}}_{m,t-1}(x) = \arg\max_a \sum_{i:\text{ans}(y_i)=a} r_t(y_i \mid x)$, with ties resolved by a fixed rule. Rollouts producing the selected answer are treated as winners, whereas those producing other answers are treated as losers when constructing $P_t(x)$. Frequency-based majority voting is recovered by assigning every trajectory unit score. At the first adaptation step, when $\pi_{t-2}$ is unavailable, we use frequency-based selection. This rule affects only preference construction and leaves Equation (35) unchanged.

**Algorithm 1** PC-Dr.DPO (Test-Time Adaptation)

**Require:** Initial policy $\pi_0$; rollout size $m$; base temperature $\beta_{\text{base}}$; cache weight $\mu$.
Initialize cache $\mathcal{C} \leftarrow \emptyset$.
**for** $t = 1, 2, \ldots, T$ **do**
  Sample mini-batch of prompts $\mathcal{B} \sim p(x)$.
  **for all** $x \in \mathcal{B}$ **do**
    Sample rollouts $\{y_i\}_{i=1}^m \sim \pi_{t-1}(\cdot \mid x)$.
    Determine the sampled pseudo-answer $\widehat{a}(x)$.
    Construct pair set $P_t(x)$ from winners vs. losers.
    Compute majority fraction $\kappa(x) = n_{\text{maj}}(x)/m$ and set $\beta_x = \beta_{\text{base}}\kappa(x)$.
    **if** $P_t(x) = \emptyset$ (degenerate) **then**
      Cache $\mathcal{C}(x) \leftarrow$ unique rollouts for $x$ (if not already cached).
    **end if**
  **end for**
  Optimize $\theta_t$ by minimizing (35).
**end for**
**return** Adapted policy $\pi_T$.

## 5 Experimental Setup

**Models.** We evaluate PC-Dr.DPO across multiple architectures and model scales, including Qwen2.5-1.5B/3B/7B-Instruct and Qwen2.5-Math-1.5B-Instruct (Qwen Team 2025). We also evaluate Llama-3.2-3B-Instruct (Meta AI 2024) to assess whether the method generalizes across model families. We use instruction-tuned variants throughout to avoid chat-template mismatches under distribution shift, ensuring that performance differences primarily reflect test-time adaptation rather than formatting artifacts.

Table 1: Test-time adaptation accuracy (%) under Avg@32 evaluation. The best result among adaptation methods is **bolded**. $*$ denotes training collapse.

| Method | Math Reasoning | | | | Knowledge Reasoning | |
|---|---|---|---|---|---|---|
| | A24 | A25 | AMC | M500 | GPQA-D | MMLU-M |
| ***Qwen2.5-1.5B-Instruct*** | | | | | | |
| Base | 2.9 | 0.8 | 22.0 | 50.7 | 24.1 | 39.5 |
| RENT | 0.0 | $*$ | 19.2 | 55.7 | $*$ | 5.2 |
| TTRL | **3.3** | $*$ | **33.6** | 62.3 | 23.5 | 10.9 |
| Co-Reward | **3.3** | $*$ | 31.4 | 59.6 | 23.3 | 10.8 |
| PC-Dr.DPO | **3.3** | $*$ | 32.3 | **62.9** | **28.8** | **45.3** |
| ***Qwen2.5-3B-Instruct*** | | | | | | |
| Base | 6.9 | 2.4 | 34.3 | 63.5 | 29.6 | 53.6 |
| RENT | $*$ | $*$ | $*$ | 56.5 | 7.8 | 46.4 |
| TTRL | **16.7** | **3.3** | 44.8 | 70.9 | **28.8** | 46.0 |
| Co-Reward | 13.1 | **3.3** | 41.0 | 69.6 | **28.8** | $*$ |
| PC-Dr.DPO | 13.3 | **3.3** | **45.8** | **73.3** | **28.8** | **64.7** |
| ***Qwen2.5-7B-Instruct*** | | | | | | |
| Base | 12.2 | 6.1 | 43.1 | 74.0 | 34.3 | 72.4 |
| RENT | 10.0 | 16.7 | 47.6 | $*$ | 33.5 | $*$ |
| TTRL | **20.0** | **17.4** | 52.7 | 79.5 | **36.9** | 76.1 |
| Co-Reward | 16.7 | 13.3 | 47.0 | 75.2 | 31.8 | 73.7 |
| PC-Dr.DPO | **20.0** | 13.3 | **53.0** | **80.3** | 35.8 | **77.2** |
| ***Qwen2.5-Math-1.5B-Instruct*** | | | | | | |
| Base | 11.1 | 8.0 | 46.8 | 73.2 | 25.8 | 55.2 |
| RENT | 15.8 | 11.5 | 48.6 | 64.8 | 25.0 | 60.8 |
| TTRL | 19.1 | **15.2** | 53.7 | 77.9 | 28.4 | 65.9 |
| Co-Reward | 17.9 | 10.0 | 49.1 | 76.9 | 27.7 | **71.0** |
| PC-Dr.DPO | **23.5** | 13.3 | **55.9** | **78.2** | **29.5** | 69.2 |
| ***Llama-3.2-3B-Instruct*** | | | | | | |
| Base | 7.4 | 0.3 | 18.5 | 40.3 | 26.4 | 43.5 |
| RENT | $*$ | $*$ | $*$ | $*$ | 16.2 | 15.4 |
| TTRL | 13.3 | $*$ | 29.9 | 57.4 | 27.9 | $*$ |
| Co-Reward | 11.0 | $*$ | 28.9 | 49.3 | 26.8 | 35.8 |
| PC-Dr.DPO | **16.7** | $*$ | **34.6** | **58.4** | **28.0** | **45.8** |

**Benchmarks.** We compare PC-Dr.DPO with three TTRL baselines: the certainty-based method RENT (Prabhudesai et al. 2025) and the ensemble-based methods TTRL and Co-Reward (Zuo et al. 2025; Zhang et al. 2025). Evaluation covers four mathematical-reasoning benchmarks—AIME24, AIME25, AMC23, and MATH500 (Hendrycks et al. 2021)—and two knowledge-intensive reasoning benchmarks, GPQA-Diamond (Rein et al. 2023) and MMLU-Pro (Wang et al. 2024). Due to computational constraints, we evaluate MMLU-Pro on its mathematics subset, which contains 1,351 examples.

Test-time adaptation is performed on the full evaluation set, or on the official test split when available. All methods use the same fixed adaptation budget for each benchmark, and we report accuracy at the final checkpoint rather than selecting the best intermediate checkpoint. This protocol avoids favoring methods that improve early but subsequently collapse, reflecting the practical setting in which the onset of degradation is not known in advance.

**Implementation details.** We implement PC-Dr.DPO in the veRL framework (Sheng et al. 2025) and run all experiments on a single node with eight NVIDIA H100 GPUs. We use Adam with a constant learning rate of $5 \times 10^{-7}$. For PC-Dr.DPO, we sample $m = 32$ rollouts per prompt and construct eight preference pairs for each policy update. For TTRL and Co-Reward, we likewise sample 32 rollouts per prompt and downsample them to eight training examples. For RENT, we directly sample eight rollouts per prompt. This keeps the number of examples entering each policy update consistent across methods. Rollouts are generated with temperature $T = 0.8$ and nucleus-sampling parameter $p = 0.9$. Additional hyperparameter settings are provided in Appendix B.1.

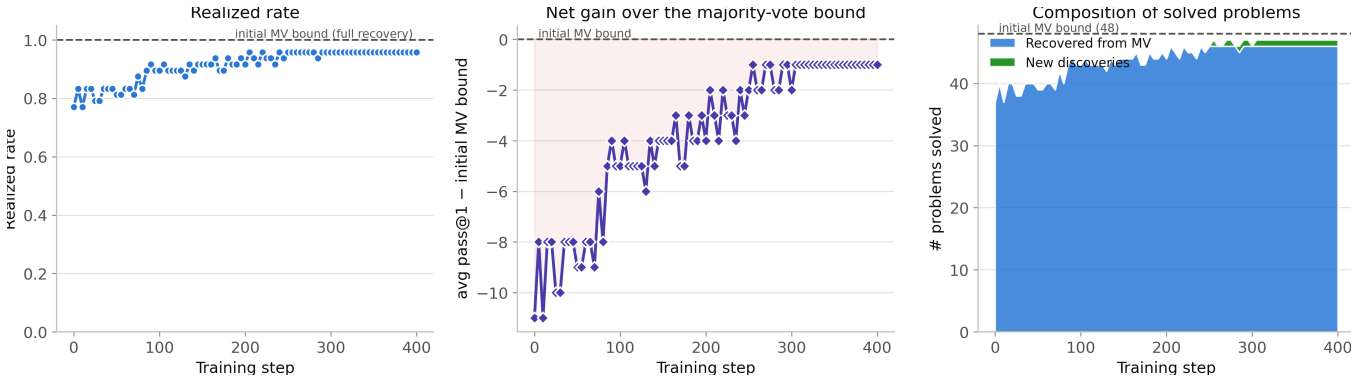



Figure 2: Adaptation dynamics of Qwen2.5-Math-1.5B-Instruct on the AMC benchmark. **Left:** fraction of problems in the initial majority-vote-solvable set that are recovered by the adapted policy. **Middle:** difference between the number of problems solved by the current policy and the initial majority-vote reference; the dashed line at zero denotes full recovery. **Right:** decomposition of the currently solved problems into those recovered from the initial majority-vote-solvable set and newly discovered solutions. The policy progressively recovers most initially available solutions while occasionally solving problems outside the initial set.

## Main Results

Table 1 reports test-time adaptation accuracy under Avg@32 evaluation. Avg@32 denotes the mean correctness over 32 sampled rollouts generated with temperature $T = 0.8$ and top-$p = 0.9$. Results marked with $*$ indicate adaptation runs that collapsed before the final checkpoint; representative failure cases are provided in Appendix C.2.

Across 24 of the 30 model–benchmark combinations, PC-Dr.DPO matches or outperforms the strongest TTRL baseline. These results demonstrate the benefit of prompt-conditional reweighting for reducing the optimization effects of finite-rollout variation during test-time adaptation.

## Ablation Studies

We conduct two ablation studies. First, we evaluate the contributions of the reliability-conditioned temperature and score-based majority selection using Qwen2.5-3B-Instruct on AMC and MATH500. Second, we study the effect of the rollout-caching mechanism using Llama-3.2-3B-Instruct on MATH500.

**Temperature and majority selection.** Table 2 isolates the two principal design choices in PC-Dr.DPO. The constant-temperature variant replaces the reliability-conditioned schedule in Equation (31) with $\beta_x = \beta_{\text{base}}$. The frequency-based variant replaces score-based majority selection with standard answer-frequency voting while retaining the adaptive temperature.

Table 2: Ablation of the reliability-conditioned temperature and score-based majority selection on Qwen2.5-3B-Instruct. We report Avg@32 accuracy (%); the best adapted result is **bolded**.

| Method | AMC | MATH500 |
|---|---|---|
| Base model | 34.3 | 63.5 |
| PC-Dr.DPO w/ constant $\beta$ | 42.0 | 72.3 |
| PC-Dr.DPO w/ frequency MV | 44.6 | 71.4 |
| PC-Dr.DPO | **45.8** | **73.3** |

We further ablate the cache-replay mechanism using Llama-3.2-3B-Instruct on MATH500. During adaptation, replaying previously cached preference groups periodically anchors the policy to earlier self-consistent solutions and mitigates self-supervised forgetting. Removing this mechanism reduces Avg@32 accuracy from $58.4\%$ to $56.3\%$. Additional analysis is provided in Appendix C.3.

## Qualitative Analysis

We analyze Qwen2.5-Math-1.5B-Instruct on AMC to better understand the dynamics of test-time adaptation under majority-vote supervision. Both TTRL and PC-Dr.DPO derive reinforcement signals from majority-voted responses among the model's own rollouts. The set of problems solved by the initial rollout majority therefore provides a useful reference for measuring how effectively adaptation converts self-consistent solutions into improved policy performance.

Empirically, we observe two distinct behaviors. For some problems, adaptation successfully recovers solutions contained in the initial majority-vote-solvable set and may additionally solve previously unsolved problems, potentially through transfer of shared reasoning structure across related prompts. For others, adaptation fails to recover the initially available solutions and may even degrade performance. We attribute this failure mode to the repeated reinforcement of incorrect population-majority pseudo-labels, which can introduce systematic bias into the adapted policy. Additional trajectories and representative examples on MATH500 across multiple model backbones are provided in Appendix C.4.

# 6 Conclusion

We analyzed majority-vote supervision in online-DPO TTRL, separating population-majority bias from prompt-dependent finite-rollout variation. To mitigate the latter, we introduced PC-Dr.DPO with reliability-conditioned within-prompt reweighting and cache replay. Across six benchmarks and five backbones, PC-Dr.DPO matches or exceeds the strongest TTRL baseline in 24 of 30 settings.

## References


Ahmadian, A.; Cremer, C.; Gallé, M.; Fadaee, M.; Kreutzer, J.; Pietquin, O.; Üstün, A.; and Hooker, S. 2024. Back to Basics: Revisiting REINFORCE Style Optimization for Learning from Human Feedback in LLMs. arXiv:2402.14740.

DeepSeek-AI. 2025. DeepSeek-R1: Incentivizing Reasoning Capability in LLMs via Reinforcement Learning. arXiv:2501.12948.

DeepSeek-AI. 2026. DeepSeek V4 Technical Documentation. https://fe-static.deepseek.com/chat/transparency/deepseek-V4-model-card-EN.pdf. Accessed: 2026-07-27.

Google. 2026. Gemini 3.5: Frontier Intelligence with Action. https://blog.google/innovation-and-ai/models-and-research/gemini-models/gemini-3-5/. Accessed: 2026-07-27.

He, B.; Zuo, Y.; Liu, Z.; Zhao, S.; Fu, Z.; Yang, J.; Qian, C.; Zhang, K.; Fan, Y.; Cui, G.; et al. 2026. How Far Can Unsupervised RLVR Scale LLM Training? *arXiv preprint arXiv:2603.08660*.

Hendrycks, D.; Burns, C.; Kadavath, S.; Arora, A.; Basart, S.; Tang, E.; Song, D.; and Steinhardt, J. 2021. Measuring mathematical problem solving with the math dataset. *arXiv preprint arXiv:2103.03874*.

Hu, J.; Liu, J. K.; Xu, H.; and Shen, W. 2025. REINFORCE++: An Efficient RLHF Algorithm with Robustness to Both Prompt and Reward Models. arXiv:2501.03262.

Ko, J.; Dingliwal, S.; Ganesh, B.; Sengupta, S.; Bodapati, S.; and Galstyan, A. 2024. SeRA: Self-Reviewing and Alignment of Large Language Models using Implicit Reward Margins. arXiv:2410.09362.

Li, Z.; Xu, T.; Zhang, Y.; Lin, Z.; Yu, Y.; Sun, R.; and Luo, Z.-Q. 2024. ReMax: A Simple, Effective, and Efficient Reinforcement Learning Method for Aligning Large Language Models. arXiv:2310.10505.

Menon, A. K.; Rawat, A. S.; Reddi, S.; Kim, S.; and Kumar, S. 2021. A statistical perspective on distillation. In *International Conference on Machine Learning*, 7632–7642. PMLR.

Meta AI. 2024. Llama 3.2: Revolutionizing Edge AI and Vision with Open, Customizable Models. https://ai.meta.com/blog/llama-3-2-connect-2024-vision-edge-mobile-devices/.

Mitchell, E. 2023. A Note on DPO with Noisy Preferences & Relationship to IPO. https://ericmitchell.ai/cdpo.pdf. Version 1.1, November 25, 2023.

Moonshot AI. 2026. Kimi K3: Open Frontier Intelligence. https://www.kimi.com/blog/kimi-k3. Accessed: 2026-07-27.

OpenAI. 2026. GPT-5.6: Frontier Intelligence That Scales with Your Ambition. https://openai.com/index/gpt-5-6/. Accessed: 2026-07-27.

Ouyang, L.; Wu, J.; Jiang, X.; Almeida, D.; Wainwright, C. L.; Mishkin, P.; Zhang, C.; Agarwal, S.; Slama, K.; Ray, A.; Schulman, J.; Hilton, J.; Kelton, F.; Miller, L.; Simens, M.; Askell, A.; Welinder, P.; Christiano, P.; Leike, J.; and Lowe, R. 2022. Training language models to follow instructions with human feedback. arXiv:2203.02155.

Pang, R. Y.; Yuan, W.; Cho, K.; He, H.; Sukhbaatar, S.; and Weston, J. 2024. Iterative Reasoning Preference Optimization. arXiv:2404.19733.

Prabhudesai, M.; Chen, L.; Ippoliti, A.; Fragkiadaki, K.; Liu, H.; and Pathak, D. 2025. Maximizing Confidence Alone Improves Reasoning. arXiv:2505.22660.

Qwen Team. 2025. Qwen2.5 Technical Report. arXiv:2412.15115.

Qwen Team. 2026. Qwen3.7. https://qwen.ai/blog?id=qwen3.7. Accessed: 2026-07-27.

Rafailov, R.; Sharma, A.; Mitchell, E.; Ermon, S.; Manning, C. D.; and Finn, C. 2024. Direct Preference Optimization: Your Language Model is Secretly a Reward Model. arXiv:2305.18290.

Rein, D.; Hou, B. L.; Stickland, A. C.; Petty, J.; Pang, R. Y.; Dirani, J.; Michael, J.; and Bowman, S. R. 2023. Gpqa: A graduate-level google-proof q&a benchmark. *arXiv preprint arXiv:2311.12022*.

Schulman, J.; Wolski, F.; Dhariwal, P.; Radford, A.; and Klimov, O. 2017. Proximal Policy Optimization Algorithms. arXiv:1707.06347.

Shao, R.; Li, S. S.; Xin, R.; Geng, S.; Wang, Y.; Oh, S.; Du, S. S.; Lambert, N.; Min, S.; Krishna, R.; Tsvetkov, Y.; Hajishirzi, H.; Koh, P. W.; and Zettlemoyer, L. 2025. Spurious Rewards: Rethinking Training Signals in RLVR. arXiv:2506.10947.

Shao, Z.; Wang, P.; Zhu, Q.; Xu, R.; Song, J.; Bi, X.; Zhang, H.; Zhang, M.; Li, Y. K.; Wu, Y.; and Guo, D. 2024. DeepSeekMath: Pushing the Limits of Mathematical Reasoning in Open Language Models. arXiv:2402.03300.

Sheng, G.; Zhang, C.; Ye, Z.; Wu, X.; Zhang, W.; Zhang, R.; Peng, Y.; Lin, H.; and Wu, C. 2025. HybridFlow: A Flexible and Efficient RLHF Framework. In *Proceedings of the Twentieth European Conference on Computer Systems*, EuroSys '25, 1279–1297. ACM.

Wang, R.; Huang, W.; Cao, Q.; Iwasawa, Y.; Matsuo, Y.; and Guo, J. 2025. Self-Harmony: Learning to Harmonize Self-Supervision and Self-Play in Test-Time Reinforcement Learning. *arXiv preprint arXiv:2511.01191*.

Wang, X.; Wei, J.; Schuurmans, D.; Le, Q.; Chi, E.; Narang, S.; Chowdhery, A.; and Zhou, D. 2023. Self-Consistency Improves Chain of Thought Reasoning in Language Models. arXiv:2203.11171.

Wang, Y.; Ma, X.; Zhang, G.; Ni, Y.; Chandra, A.; Guo, S.; Ren, W.; Arulraj, A.; He, X.; Jiang, Z.; et al. 2024. Mmlu-pro: A more robust and challenging multi-task language understanding benchmark. *Advances in Neural Information Processing Systems*, 37: 95266–95290.

Wu, J.; Xie, Y.; Yang, Z.; Wu, J.; Chen, J.; Gao, J.; Ding, B.; Wang, X.; and He, X. 2025a. Towards Robust Alignment of Language Models: Distributionally Robustifying Direct Preference Optimization. arXiv:2407.07880.

Wu, M.; Zhang, Z.; Dong, Q.; Xi, Z.; Zhao, J.; Jin, S.; Fan, X.; Zhou, Y.; Lv, H.; Zhang, M.; Fu, Y.; Liu, Q.; Zhang, S.; and

Zhang, Q. 2025b. Reasoning or Memorization? Unreliable Results of Reinforcement Learning Due to Data Contamination. arXiv:2507.10532.

Yu, Q.; Zhang, Z.; Zhu, R.; Yuan, Y.; Zuo, X.; Yue, Y.; Dai, W.; Fan, T.; Liu, G.; Liu, L.; Liu, X.; Lin, H.; Lin, Z.; Ma, B.; Sheng, G.; Tong, Y.; Zhang, C.; Zhang, M.; Zhang, W.; Zhu, H.; Zhu, J.; Chen, J.; Chen, J.; Wang, C.; Yu, H.; Song, Y.; Wei, X.; Zhou, H.; Liu, J.; Ma, W.-Y.; Zhang, Y.-Q.; Yan, L.; Qiao, M.; Wu, Y.; and Wang, M. 2025. DAPO: An Open-Source LLM Reinforcement Learning System at Scale. arXiv:2503.14476.

Zhang, Z.; Zhu, J.; Ge, X.; Zhao, Z.; Zhou, Z.; Li, X.; Feng, X.; Yao, J.; and Han, B. 2025. Co-reward: Self-supervised reinforcement learning for large language model reasoning via contrastive agreement. *arXiv e-prints*, arXiv–2508.

Zhao, X.; Kang, Z.; Feng, A.; Levine, S.; and Song, D. 2025. Learning to Reason without External Rewards. arXiv:2505.19590.

Zheng, C.; Liu, S.; Li, M.; Chen, X.-H.; Yu, B.; Gao, C.; Dang, K.; Liu, Y.; Men, R.; Yang, A.; Zhou, J.; and Lin, J. 2025. Group Sequence Policy Optimization. arXiv:2507.18071.

Zuo, Y.; Zhang, K.; Sheng, L.; Qu, S.; Cui, G.; Zhu, X.; Li, H.; Zhang, Y.; Long, X.; Hua, E.; Qi, B.; Sun, Y.; Ma, Z.; Yuan, L.; Ding, N.; and Zhou, B. 2025. TTRL: Test-Time Reinforcement Learning. arXiv:2504.16084.

# A Detailed Proofs

## KL-DRO Derivation and Gradient Behavior

Let $s = (x, y_w, y_l)$ denote a preference sample and recall

$$g_\theta(s) = \log \frac{\pi_\theta(y_w \mid x)}{\pi_{\text{ref}}(y_w \mid x)} - \log \frac{\pi_\theta(y_l \mid x)}{\pi_{\text{ref}}(y_l \mid x)}, \qquad \nu_\theta(s) = \sigma(\tau g_\theta(s)), \qquad h_\theta(s) = \log \nu_\theta(s). \tag{37}$$

Let $p$ denote the empirical distribution over the preference pairs.

**KL-constrained formulation.** Consider the distributionally robust score

$$\sup_{q:\, \mathrm{KL}(q\|p)\le\eta} \mathbb{E}_{s\sim q}\left[h_\theta(s)\right], \tag{38}$$

where $\eta \ge 0$ controls the allowable deviation from $p$. Assume $q \ll p$ and let $r = dq/dp$ be the corresponding density ratio. Then $r \ge 0$, $\mathbb{E}_p[r] = 1$, and

$$\mathrm{KL}(q\|p) = \mathbb{E}_p[r \log r] = \mathbb{E}_p[\phi(r)], \qquad \phi(r) := r\log r - r + 1.$$

Hence, Equation (38) is equivalent to

$$\sup_{r\ge 0} \mathbb{E}_p[r h_\theta] \quad \text{s.t.} \quad \mathbb{E}_p[\phi(r)] \le \eta, \qquad \mathbb{E}_p[r] = 1. \tag{39}$$

Introduce a multiplier $\beta \ge 0$ for the divergence constraint and $\alpha \in \mathbb{R}$ for the normalization constraint. The Lagrangian is

$$\begin{aligned}\mathcal{L}(r,\alpha,\beta) &= \mathbb{E}_p[r h_\theta] - \beta\big(\mathbb{E}_p[\phi(r)] - \eta\big) + \alpha\big(\mathbb{E}_p[r] - 1\big) \\ &= \beta\eta - \alpha + \beta\,\mathbb{E}_p\left[r\frac{h_\theta + \alpha}{\beta} - \phi(r)\right].\end{aligned} \tag{40}$$

For $\beta > 0$, the convex conjugate of $\phi(r) = r\log r - r + 1$ is

$$\phi^*(u) = \sup_{r\ge 0}\{ru - \phi(r)\} = e^u - 1,$$

with maximizer $r^*(u) = e^u$. Maximizing Equation (40) over $r$ therefore gives

$$g(\alpha,\beta) = \beta\eta - \alpha + \beta\,\mathbb{E}_p\left[e^{(h_\theta+\alpha)/\beta} - 1\right]. \tag{41}$$

Differentiating with respect to $\alpha$ yields

$$-1 + \mathbb{E}_p\left[e^{(h_\theta+\alpha)/\beta}\right] = 0,$$

and thus

$$\alpha^* = -\beta \log \mathbb{E}_p\left[e^{h_\theta/\beta}\right]. \tag{42}$$

Substituting Equation (42) into Equation (41) gives

$$\sup_{q:\, \mathrm{KL}(q\|p)\le\eta} \mathbb{E}_q[h_\theta] = \inf_{\beta>0}\left\{\beta\eta + \beta\log \mathbb{E}_p\left[e^{h_\theta/\beta}\right]\right\}. \tag{43}$$

For any $\beta > 0$, the associated exponentially tilted distribution is

$$q_{\theta,\beta}(s) = p(s)\frac{\exp(h_\theta(s)/\beta)}{\mathbb{E}_{s'\sim p}\left[\exp(h_\theta(s')/\beta)\right]}. \tag{44}$$

Under the fixed-temperature approximation, we associate each prescribed robustness radius $\eta$ with a temperature $\beta^\star(\eta)$, which is treated as independent of $\theta$ and held fixed during the policy update.

**Fixed-temperature objective.** Assume that $\beta^\star(\eta)$ minimizes the dual objective in Equation (43) under this fixed-temperature parameterization. Then

$$\sup_{q:\, \mathrm{KL}(q\|p)\le\eta} \mathbb{E}_q[h_\theta] = \beta^\star(\eta)\eta + \beta^\star(\eta)\log \mathbb{E}_{s\sim p}\left[\exp\left(\frac{h_\theta(s)}{\beta^\star(\eta)}\right)\right]. \tag{45}$$

Because $\eta$ and $\beta^\star(\eta)$ are fixed during the policy update, the term $\beta^\star(\eta)\eta$ is independent of $\theta$ and can be omitted. Writing $\beta = \beta^\star(\eta)$ and negating the remaining robust score gives the Dr.DPO loss

$$\mathcal{L}_{\text{DrDPO}}(\theta) = -\beta \log \mathbb{E}_{s\sim p}\left[\exp\left(\frac{h_\theta(s)}{\beta}\right)\right]. \tag{46}$$

**Gradient.** Define

$$w_\beta(s) := \frac{\exp(h_\theta(s)/\beta)}{\mathbb{E}_{s'\sim p}\left[\exp(h_\theta(s')/\beta)\right]}. \tag{47}$$

Since

$$\nabla_\theta h_\theta(s) = \tau\big(1 - \nu_\theta(s)\big)\nabla_\theta g_\theta(s), \tag{48}$$

differentiating Equation (46) gives

$$\nabla_\theta \mathcal{L}_{\text{DrDPO}}(\theta) = -\tau\,\mathbb{E}_{s\sim p}\left[w_\beta(s)\big(1-\nu_\theta(s)\big)\nabla_\theta g_\theta(s)\right]. \tag{49}$$

**Effect of the temperature.** Consider a finite collection of preference pairs $\mathcal{S} = \{s_i\}_{i=1}^N$ and let

$$\nu_i := \nu_\theta(s_i).$$

The normalized exponentially tilted weights are

$$\overline{w}_i(\beta) = \frac{\nu_i^{1/\beta}}{\sum_{k=1}^N \nu_k^{1/\beta}}. \tag{50}$$

The corresponding gradient is

$$\nabla_\theta \mathcal{L}(\theta) = -\tau \sum_{i=1}^N \overline{w}_i(\beta)\big(1-\nu_i\big)\nabla_\theta g_\theta(s_i). \tag{51}$$

Define the weighted residual logistic factor

$$A(\beta) := \sum_{i=1}^N \overline{w}_i(\beta)\big(1-\nu_i\big) = 1 - \sum_{i=1}^N \overline{w}_i(\beta)\nu_i. \tag{52}$$

Let $t = 1/\beta$. Then

$$\overline{w}_i(t) = \frac{\exp(t\log\nu_i)}{\sum_{k=1}^N \exp(t\log\nu_k)}.$$

Differentiating the weighted mean of $\nu_i$ gives

$$\frac{d}{dt}\sum_{i=1}^N \overline{w}_i(t)\nu_i = \mathrm{Cov}_{\overline{w}(t)}\left(\nu_i, \log\nu_i\right) \ge 0, \tag{53}$$

where the inequality follows because $\log\nu$ is increasing in $\nu$. Consequently, $A(\beta)$ is nondecreasing in $\beta$, or equivalently, decreases as $\beta$ decreases.

If the pairwise margin gradients satisfy

$$\|\nabla_\theta g_\theta(s_i)\| \le G \qquad \text{for all } i,$$

then

$$\|\nabla_\theta \mathcal{L}(\theta)\| \le \tau G\, A(\beta). \tag{54}$$

Thus, decreasing $\beta$ decreases an upper bound on the update magnitude.

## Proof of Theorem 1

We first restate the uniform empirical-Bernstein result used in the proof.

**Lemma** (Uniform empirical-Bernstein bound; adapted from (Menon et al. 2021))**.** *Let $\ell : \{0,1\} \times \mathbb{R} \to [0,1]$, let $\mathcal{F}$ be a class of predictors $f : \mathcal{S} \to \mathbb{R}$, and let $a : \mathcal{S} \to \Delta_2$ be a fixed measurable map. Define*

$$\ell(f(s)) := \begin{pmatrix} \ell(1, f(s)) \\ \ell(0, f(s)) \end{pmatrix}$$

*and the induced loss class*

$$\mathcal{H}_a := \left\{ h_f^a : \mathcal{S} \to [0,1] \;\middle|\; h_f^a(s) = a(s)^\top \ell(f(s)),\ f \in \mathcal{F} \right\}.$$

*Let*

$$\mathcal{M}_N(a) := \mathcal{N}_\infty\left(\frac{1}{N}, \mathcal{H}_a, 2N\right),$$

*where $\mathcal{N}_\infty(\epsilon, \mathcal{H}, m)$ denotes the uniform $\ell_\infty$ covering number of $\mathcal{H}$ on $m$ points.*

*For a sample $S = \{s_n\}_{n=1}^N$, define*

$$\widehat{R}_a(f; S) := \frac{1}{N} \sum_{n=1}^{N} a(s_n)^\top \ell(f(s_n)), \tag{55}$$

*and let*

$$\mathbb{V}_{N,a}(f; S) := \frac{1}{N} \sum_{n=1}^{N} \left( a(s_n)^\top \ell(f(s_n)) - \widehat{R}_a(f; S) \right)^2. \tag{56}$$

*Then, for any $\delta \in (0,1)$, with probability at least $1-\delta$ over $S \sim \mathcal{P}^N$, every $f \in \mathcal{F}$ satisfies*

$$\begin{aligned} \mathbb{E}_{s\sim\mathcal{P}}\left[a(s)^\top \ell(f(s))\right] \le \widehat{R}_a(f; S) \\ + O\left( \sqrt{\frac{\mathbb{V}_{N,a}(f; S) \log(\mathcal{M}_N(a)/\delta)}{N}} \right. \\ \left. + \frac{\log(\mathcal{M}_N(a)/\delta)}{N} \right). \end{aligned} \tag{57}$$

*Proof of Theorem 1.* For a preference sample $s = (x, y_w, y_l)$, write

$$\ell(f(s)) := \begin{pmatrix} \ell(1, f(s)) \\ \ell(0, f(s)) \end{pmatrix} \in [0,1]^2.$$

Let $p^*(s), \hat{p}(s) \in \Delta_2$ denote the true and pseudo-preference distributions associated with $s$, respectively.

Define the true population risk, pseudo-preference population risk, and pseudo-preference empirical risk by

$$R(f) := \mathbb{E}_{s\sim\mathcal{P}}\left[p^*(s)^\top \ell(f(s))\right], \tag{58}$$

$$\widetilde{R}(f) := \mathbb{E}_{s\sim\mathcal{P}}\left[\hat{p}(s)^\top \ell(f(s))\right], \tag{59}$$

$$\widetilde{R}(f; S) := \frac{1}{N} \sum_{n=1}^{N} \hat{p}(s_n)^\top \ell(f(s_n)). \tag{60}$$

Consider the induced pseudo-preference loss class

$$\widetilde{\mathcal{H}} := \left\{ \widetilde{h}_f : \mathcal{S} \to [0,1] \;\middle|\; \widetilde{h}_f(s) = \hat{p}(s)^\top \ell(f(s)),\ f \in \mathcal{F} \right\},$$

and define

$$\widetilde{\mathcal{M}}_N := \mathcal{N}_\infty\left(\frac{1}{N}, \widetilde{\mathcal{H}}, 2N\right).$$

Because $\hat{p}(s) \in \Delta_2$ and $\ell(f(s)) \in [0,1]^2$, every function in $\widetilde{\mathcal{H}}$ takes values in $[0,1]$.

Let $\widetilde{\mathbb{V}}_N(f; S)$ denote the empirical variance of

$$\left\{ \hat{p}(s_n)^\top \ell(f(s_n)) \right\}_{n=1}^N.$$

Applying the empirical-Bernstein bound with $a(s) = \hat{p}(s)$ gives that, with probability at least $1-\delta$ over $S \sim \mathcal{P}^N$, every $f \in \mathcal{F}$ satisfies

$$\begin{aligned} \widetilde{R}(f) \le \widetilde{R}(f; S) \\ + O\left( \sqrt{\frac{\widetilde{\mathbb{V}}_N(f; S) \log(\widetilde{\mathcal{M}}_N/\delta)}{N}} \right. \\ \left. + \frac{\log(\widetilde{\mathcal{M}}_N/\delta)}{N} \right). \end{aligned} \tag{61}$$

It remains to control the discrepancy between the true and pseudo-preference population risks. Let

$$d(s) := \hat{p}(s) - p^*(s) = \begin{pmatrix} d_1(s) \\ d_0(s) \end{pmatrix}.$$

Since both $\hat{p}(s)$ and $p^*(s)$ are probability vectors,

$$d_1(s) + d_0(s) = 0.$$

Therefore,

$$\begin{aligned} \left| d(s)^\top \ell(f(s)) \right| &= \left| d_1(s)\ell(1, f(s)) + d_0(s)\ell(0, f(s)) \right| \\ &= \left| d_1(s) \left( \ell(1, f(s)) - \ell(0, f(s)) \right) \right| \\ &\le |d_1(s)| \\ &= \frac{1}{2} \left( |d_1(s)| + |d_0(s)| \right) \\ &= \frac{1}{2} \left\| \hat{p}(s) - p^*(s) \right\|_1. \end{aligned} \tag{62}$$

The inequality follows from $\ell(1, f(s)), \ell(0, f(s)) \in [0,1]$, which implies

$$|\ell(1, f(s)) - \ell(0, f(s))| \le 1.$$

Taking expectations in Equation (62) yields

$$\begin{aligned} \left| \widetilde{R}(f) - R(f) \right| &= \left| \mathbb{E}_{s\sim\mathcal{P}} \left[ \left( \hat{p}(s) - p^*(s) \right)^\top \ell(f(s)) \right] \right| \\ &\le \mathbb{E}_{s\sim\mathcal{P}} \left[ \left| \left( \hat{p}(s) - p^*(s) \right)^\top \ell(f(s)) \right| \right] \\ &\le \frac{1}{2} \mathbb{E}_{s\sim\mathcal{P}} \left[ \left\| \hat{p}(s) - p^*(s) \right\|_1 \right]. \end{aligned} \tag{63}$$

Consequently,

$$R(f) \le \widetilde{R}(f) + \frac{1}{2} \mathbb{E}_{s\sim\mathcal{P}} \left[ \left\| \hat{p}(s) - p^*(s) \right\|_1 \right]. \tag{64}$$

□

## Total-Variation Identity for Deterministic Binary Preferences

**Lemma** (Total-variation identity for deterministic binary preferences)**.** *Assume both the true and pseudo-preference distributions are deterministic. Then*

$$\frac{1}{2}\left\|\hat{p}(s)-p^*(s)\right\|_1 = \mathbf{1}\left\{\widehat{a}_{m,b}(x)\neq a^\star(x)\right\}. \tag{65}$$

*Consequently,*

$$\frac{1}{2}\mathbb{E}_{s\sim\mathcal{P}}\left[\left\|\hat{p}(s)-p^*(s)\right\|_1\right] = \mathbb{E}_x\left[U_{m,b}(x)\right]. \tag{66}$$

*Proof.* Let $z^*(s)\in\{0,1\}$ denote the true preference label and let $\widehat{z}(s)\in\{0,1\}$ denote the pseudo-preference label induced by the sampled-majority answer. Under the deterministic binary construction,

$$p^*(s)=e_{z^*(s)}, \qquad \hat{p}(s)=e_{\widehat{z}(s)},$$

where $e_0=(1,0)^\top$ and $e_1=(0,1)^\top$. Hence,

$$\begin{aligned}\frac{1}{2}\left\|\hat{p}(s)-p^*(s)\right\|_1 &= \frac{1}{2}\left\|e_{\widehat{z}(s)}-e_{z^*(s)}\right\|_1\\ &= \mathbf{1}\left\{\widehat{z}(s)\neq z^*(s)\right\}\\ &= \mathbf{1}\left\{\widehat{a}_{m,b}(x)\neq a^\star(x)\right\}. \end{aligned}\tag{67}$$

Taking expectations and applying the law of total expectation gives

$$\begin{aligned}\frac{1}{2}\mathbb{E}_{s\sim\mathcal{P}}\left[\left\|\hat{p}(s)-p^*(s)\right\|_1\right] &= \mathbb{E}_x\left[\Pr(\widehat{a}_{m,b}(x)\neq a^\star(x)\mid x)\right]\\ &= \mathbb{E}_x\left[U_{m,b}(x)\right]. \end{aligned}\tag{68}$$

□

## Proof of Majority-Vote Concentration

*Proof.* Fix a prompt $x$ and let

$$Z_i := \mathbf{1}\left\{\mathrm{ans}(y_i)=a^\star(x)\right\}, \qquad y_i \overset{\text{i.i.d.}}{\sim} \pi_b(\cdot\mid x),$$

for $i=1,\dots,m$. Conditional on $x$, the variables $Z_1,\dots,Z_m$ are i.i.d. Bernoulli random variables satisfying

$$\mathbb{E}[Z_i\mid x]=\rho_b(x).$$

Define their empirical mean by

$$\overline{Z}_m := \frac{1}{m}\sum_{i=1}^m Z_i.$$

Under the binary-answer abstraction, if $\rho_b(x)>1/2$, then the population-majority answer is $a^\star(x)$. Therefore, disagreement between the sampled and population majorities implies $\overline{Z}_m\le 1/2$. Hence, Hoeffding's inequality gives

$$\begin{aligned}V_{m,b}(x) &\le \Pr\left(\overline{Z}_m\le\frac{1}{2}\mid x\right)\\ &= \Pr\left(\overline{Z}_m-\rho_b(x)\le -\left(\rho_b(x)-\frac{1}{2}\right)\middle| x\right)\\ &\le \exp\left(-2m\left(\rho_b(x)-\frac{1}{2}\right)^2\right). \end{aligned}\tag{69}$$

If instead $\rho_b(x)<1/2$, then the population-majority answer is incorrect. Disagreement with that population majority implies $\overline{Z}_m\ge 1/2$, and Hoeffding's inequality yields

$$\begin{aligned}V_{m,b}(x) &\le \Pr\left(\overline{Z}_m\ge\frac{1}{2}\mid x\right)\\ &= \Pr\left(\overline{Z}_m-\rho_b(x)\ge\frac{1}{2}-\rho_b(x)\middle| x\right)\\ &\le \exp\left(-2m\left(\frac{1}{2}-\rho_b(x)\right)^2\right). \end{aligned}\tag{70}$$

For even $m$, these inclusions remain valid under any deterministic tie-breaking rule. Combining the two cases gives

$$V_{m,b}(x)\le\exp\left(-2m\left|\rho_b(x)-\frac{1}{2}\right|^2\right).$$

For completeness, under the binary abstraction,

$$U_{m,b}(x)=B_b(x)+\big(1-2B_b(x)\big)V_{m,b}(x).$$

Thus, when $\rho_b(x)\ge 1/2+\gamma$, we have $B_b(x)=0$ and

$$U_{m,b}(x)=V_{m,b}(x)\le e^{-2m\gamma^2}.$$

When $\rho_b(x)\le 1/2-\gamma$, we have $B_b(x)=1$ and

$$U_{m,b}(x)=1-V_{m,b}(x)\ge 1-e^{-2m\gamma^2}.$$

□

## Proof of Bias–Variation Separation

*Proof.* Under the binary-answer abstraction, the exact majority-error decomposition gives

$$U_{m,b}(x)-B_b(x)=\big(1-2B_b(x)\big)V_{m,b}(x), \tag{71}$$

where

$$B_b(x)=\mathbf{1}\left\{\rho_b(x)<\frac{1}{2}\right\}.$$

Since $B_b(x)\in\{0,1\}$, we have $|1-2B_b(x)|=1$, and therefore

$$|U_{m,b}(x)-B_b(x)|=V_{m,b}(x). \tag{72}$$

Define

$$\alpha_b := \mathbb{E}_x[B_b(x)]=\Pr_x\left(\rho_b(x)<\frac{1}{2}\right).$$

Under the uniform gap assumption

$$\left|\rho_b(x)-\frac{1}{2}\right|\ge\gamma \qquad \text{almost surely,}$$

the majority-vote concentration result proved above yields

$$V_{m,b}(x)\le e^{-2m\gamma^2} \qquad \text{almost surely.}$$

Hence,

$$\begin{aligned}\left|\mathbb{E}_x[U_{m,b}(x)]-\alpha_b\right| &= \left|\mathbb{E}_x\left[U_{m,b}(x)-B_b(x)\right]\right|\\ &\le \mathbb{E}_x\left[\left|U_{m,b}(x)-B_b(x)\right|\right]\\ &= \mathbb{E}_x[V_{m,b}(x)]\\ &\le e^{-2m\gamma^2}. \end{aligned}\tag{73}$$

Table 3: Hyperparameters used in our experiments.

| Hyperparameter | Value |
|---|---|
| Max prompt length | 1,024 |
| Max response length | 3,072 |
| Training batch size | 24 AIME24<br>24 AIME25<br>16 AMC<br>32 MATH500<br>16 GPQA-Diamond<br>32 MMLU-Pro Math |
| Dataset size | 30 AIME24<br>30 AIME25<br>83 AMC<br>500 MATH500<br>198 GPQA-Diamond<br>1,351 MMLU-Pro Math |
| Total epochs | 240 AIME24<br>240 AIME25<br>80 AMC<br>40 MATH500<br>40 GPQA-Diamond<br>80 MMLU-Pro Math |
| PPO mini-batch size | 4 |
| PPO micro-batch size | 8 |
| Optimizer | Adam |
| Learning rate | $5 \times 10^{-7}$ |
| DPO inverse temperature $\tau$ | 0.1 |
| Base DRO temperature $\beta_{\text{base}}$ | 2 |
| Preference pairs per prompt | 8 |
| Rollout scoring strategy | `implicit_dpo_reward` |
| Pair-construction strategy | `random` |
| Training rollouts per prompt | 32 |
| Training sampling | Temperature: 0.8<br>Top-$p$: 0.9<br>Top-$k$: $-1$ |
| Validation rollouts per prompt | 32 |
| Validation sampling | Temperature: 0.8<br>Top-$p$: 0.9<br>Top-$k$: $-1$ |

In particular,

$$\mathbb{E}_x[U_{m,b}(x)] \le \alpha_b + e^{-2m\gamma^2}. \tag{74}$$

The majority-vote generalization bound gives, with probability at least $1-\delta$ over $S \sim \mathcal{P}^N$, simultaneously for every $f \in \mathcal{F}$,

$$R(f) \le \widetilde{R}(f;S) + \mathbb{E}_x[U_{m,b}(x)] + \mathcal{G}_N(f,\delta;S).$$

Substituting Equation (74) yields

$$R(f) \le \widetilde{R}(f;S) + \alpha_b + e^{-2m\gamma^2} + \mathcal{G}_N(f,\delta;S),$$

which proves the result. □

# B Implementation Details

## Hyperparameters

For PC-Dr.DPO, `ppo_micro_batch_size` is set equal to the number of preference pairs constructed per prompt, ensuring that each prompt group remains intact during within-prompt robust reweighting.

# C More Results

## Effect of the Rollout Count

Figure 3 compares rollout counts $m \in \{16, 32, 64\}$ for Qwen2.5-Math-1.5B-Instruct on AMC. Larger rollout counts reduce variation in the sampled pseudo-labels and yield more stable validation trajectories. This observation is consistent with our analysis: increasing $m$ suppresses finite-rollout variation.

## Self-Reinforcing Collapse under Incorrect Population Majorities

Figure 4 shows the adaptation dynamics of Qwen2.5-1.5B-Instruct on AIME25. The sampled pseudo-label accuracy remains close to zero, indicating that most prompt-level supervision signals are incorrect. Nevertheless, the modal-answer fraction increases throughout training and eventually approaches one. The policy therefore becomes more internally consistent without becoming more correct. Repeated optimization against these increasingly decisive but incorrect pseudo-labels reinforces population-majority bias, while validation Avg@32 accuracy ultimately collapses to zero.

## Analysis of Cache Replay

Figure 5 examines the cache-replay mechanism using Llama-3.2-3B-Instruct on MATH500. During adaptation, the cache accumulates preference groups associated with previously mastered prompts and periodically replays them in subsequent updates. As shown in Figure 5(a), replay events revisit a subset of these earlier solutions throughout training.

Figures 5(b)–(c) compare adaptation with and without cache replay. Without replay, pseudo-label accuracy gradually decreases and validation performance exhibits larger regressions. Replaying cached preference groups anchors the policy to earlier self-consistent solutions, improving the retention of previously acquired behavior and raising final Avg@32 accuracy from $56.3\%$ to $58.4\%$. These results support the use of cache replay as a mechanism for mitigating self-supervised forgetting during online adaptation.

## Additional Adaptation Dynamics on MATH500

Figure 6 presents additional adaptation trajectories on MATH500 for Llama-3.2-3B-Instruct and Qwen2.5-Math-1.5B-Instruct. For each run, the problems solved by the initial rollout majority define a fixed reference set. The left panels report the fraction of this set recovered by the current policy, the middle panels show the difference between the current number of solved problems and the initial majority-vote reference, and the right panels decompose the currently solved problems into recovered and newly discovered solutions.

Across both backbones, adaptation progressively recovers most solutions available in the initial reference set. Llama-3.2-3B-Instruct recovers approximately $90\%$ of the initially solvable problems, whereas Qwen2.5-Math-1.5B-Instruct approaches nearly complete recovery. Both models also solve some problems outside the initial reference set, showing that the initial majority-vote-solvable set is not a strict performance upper bound. Nevertheless, incomplete

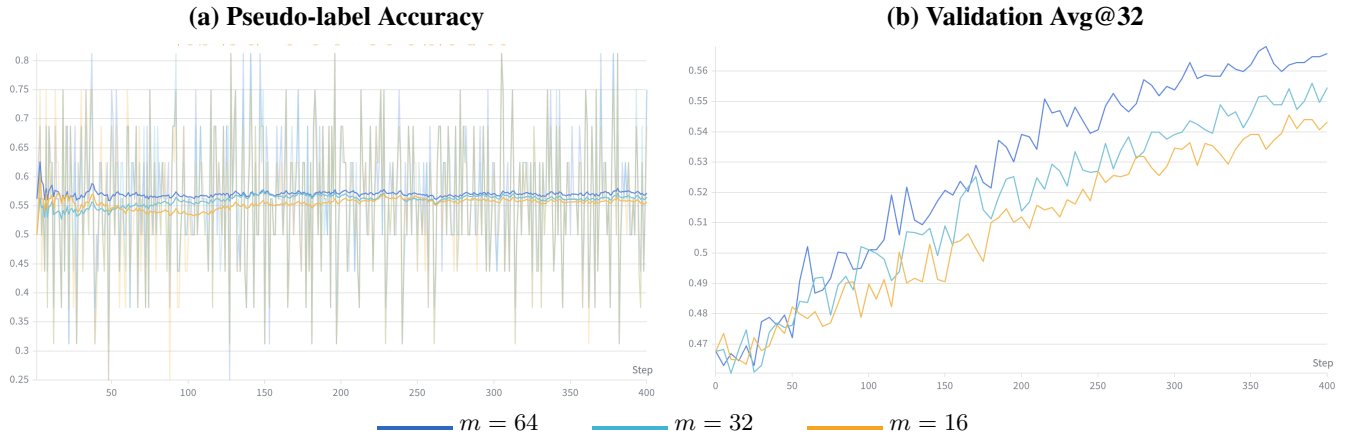



Figure 3: Effect of the rollout count $m$ during test-time adaptation of Qwen2.5-Math-1.5B-Instruct on AMC. **Left:** pseudo-label accuracy across adaptation steps. The faint trajectories show the per-step measurements, while the darker curves show their smoothed trends. **Right:** validation Avg@32 accuracy throughout adaptation. Increasing $m$ reduces the variability of sampled pseudo-labels and produces more stable downstream improvement.

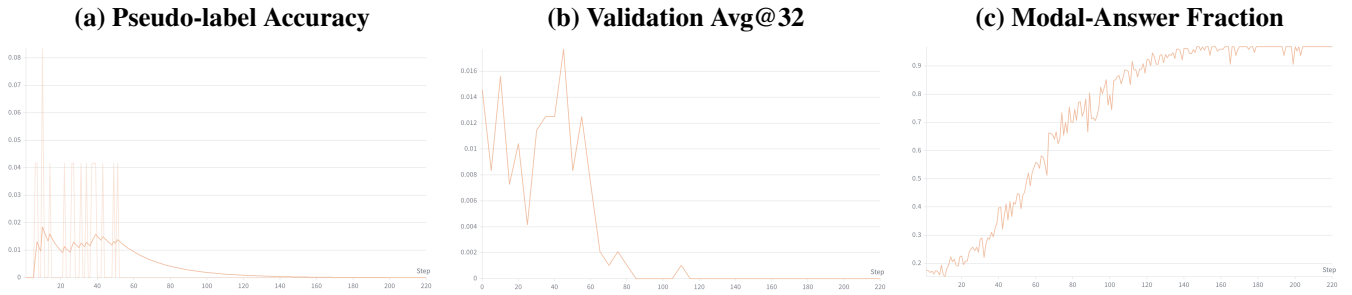



Figure 4: Self-reinforcing collapse of Qwen2.5-1.5B-Instruct during test-time adaptation on AIME25. **Left:** accuracy of the sampled pseudo-labels relative to the ground-truth answers. **Middle:** validation Avg@32 accuracy, which eventually decreases to zero. **Right:** average modal-answer fraction within each rollout group. Although the modal-answer fraction steadily approaches one, the pseudo-label accuracy remains close to zero. Thus, the policy becomes increasingly confident in predominantly incorrect pseudo-labels, reinforcing systematic population-majority bias and ultimately producing adaptation collapse.

recovery remains, indicating that some initially available solutions are lost during adaptation. These trajectories illustrate the competing effects of solution recovery, cross-prompt transfer, and degradation induced by systematic pseudo-label errors, which can steer policy updates away from previously available solutions.

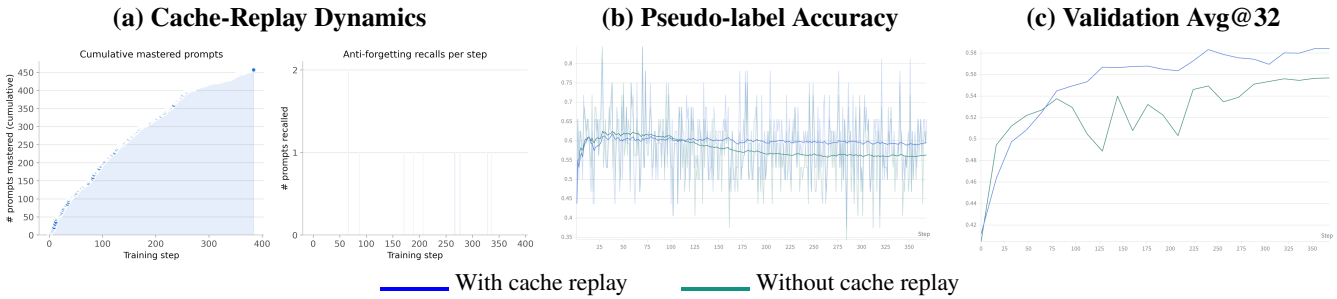



Figure 5: Effect of cache replay during adaptation of Llama-3.2-3B-Instruct on MATH500. **Left:** cache-replay dynamics, including the cumulative number of prompts whose solutions have been cached and the number of previously mastered prompts recalled at each adaptation step. **Middle:** pseudo-label accuracy with and without cache replay; faint curves show per-step values and darker curves show smoothed trajectories. **Right:** validation Avg@32 accuracy throughout adaptation. Cache replay periodically revisits earlier self-consistent solutions, reducing degradation in pseudo-label quality and mitigating self-supervised forgetting. Removing cache replay lowers final Avg@32 accuracy from $58.4\%$ to $56.3\%$.

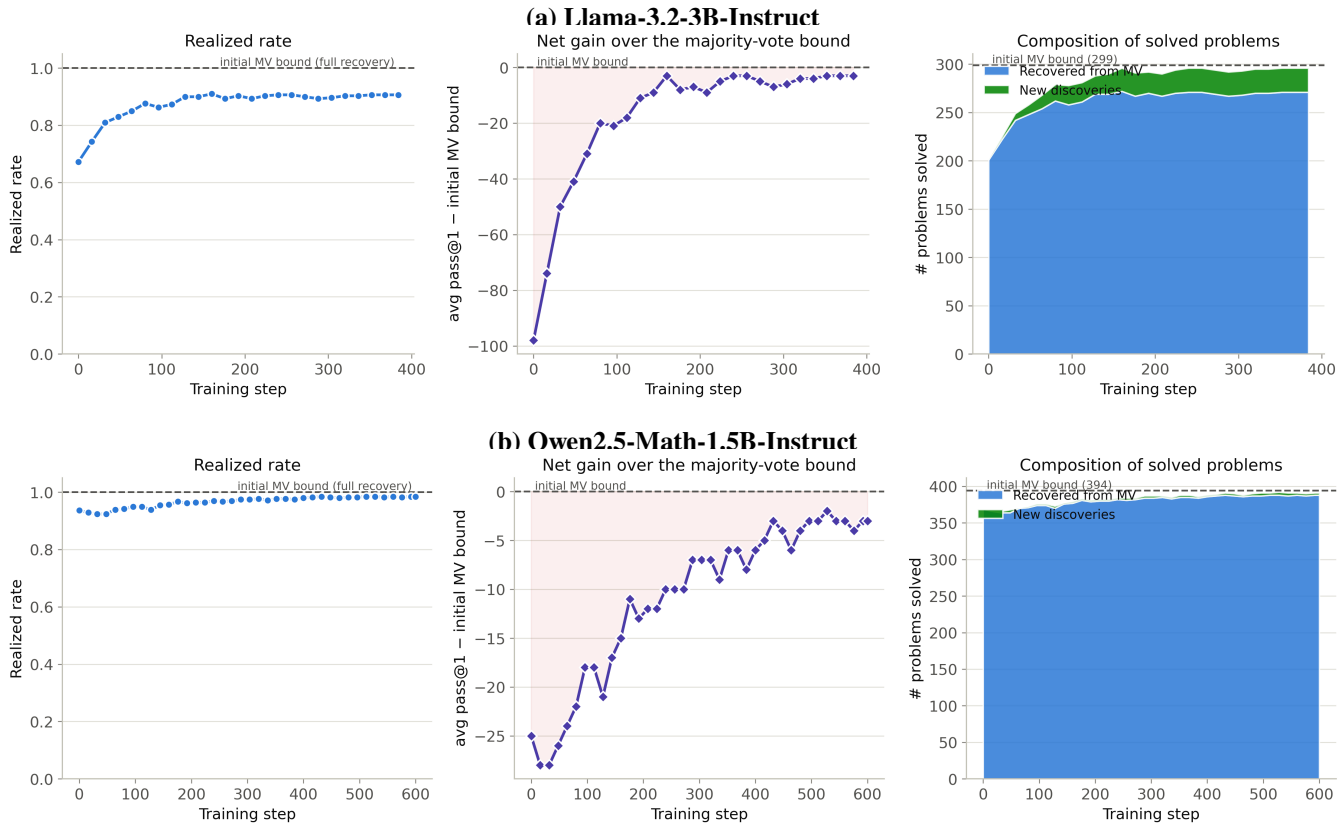



Figure 6: Additional adaptation dynamics on MATH500 for Llama-3.2-3B-Instruct and Qwen2.5-Math-1.5B-Instruct. In each row, the problems solved by the initial rollout majority define a fixed reference set. **Left:** fraction of this initial set recovered by the current policy. **Middle:** difference between the number of problems solved by the current policy and the initial majority-vote reference; the dashed line at zero denotes full numerical recovery of the initial reference level. **Right:** decomposition of the currently solved problems into solutions recovered from the initial reference set and newly discovered solutions. Both backbones recover most initially available solutions and occasionally solve problems outside the initial reference set, while incomplete recovery indicates degradation induced by systematic pseudo-label errors.